2P5-3

Deep-leaning quantitative imaging regarding ultrasonic echoic and attenuation properties

Kaichen Hua, Yiran Li, Mengfei Zhang and Chikayoshi Sumi†
(Grad. Sch. of Sophia Univ.)

1. Introduction

We are conducting research on quantitative imaging of reverberation and attenuation characteristics in ultrasonic echoes using deep learning (DL) techniques[1]. Specifically, for dealing with reverberation, we use methods such as the DDSRCNN (Deep De-Noising Super-Resolution CNN)[1] to perform so-called inverse filtering, and the CAE (Convolutional AutoEncoder)[1] to perform speckle reduction. We also use FSRCNN, TecoGAN, and among others for superresolution[2]. We have been reporting that the superresolution and speckle reduction are effective for preprocessing each other and with respect to segmentation[2,3].

In this study, we performed the inverse filtering with a simple supervised convolution neural network (CNN) to examine the performance to be yielded by the only convolutional model. Moreover, attenuation estimation was also performed with the CNN. We also performed the speckle reduction by our developed supervised CAE and compare the performance with that yielded by the unsupervised CAE[1]. A laboratory-made simulator[2,3] was used to generate simulated echo data.

2. Methods

2.1 Simulated echo data

The simulation data of the echo was generated with our made simulator by convolving the acoustic impulse response with the tissue echoic characteristics.

In this study, a soft tissue model was used, which includes a vascular lumen model, with a circular cross-section of 2.5 mm in diameter, containing low-intensity random scatterers such as red blood cells in blood with a typical inherent acoustic impedance of 1.61×10^6 kg/m^{2}s, and the soft tissue itself has a typical inherent acoustic impedance ranging from 1.65 to 1.69×10^6 kg/m^{2}s randomly and random backscatter coefficients.

The reflection and transmission coefficients at the boundary between the tissues were calculated based on the ultrasonic propagation direction and the inherent acoustic impedances. While the backscatter coefficients could be modeled to have a directivity, here they were simply modeled as positive and negative random numbers.

The acoustic impulse response was modeled with the 3 type point spread functions (PSFs), i.e., the Gaussian-, parabolic and rectangular type PSFs, with a center frequency of 7.5 MHz.
The energy of the parabolic type PSF was made same as that of the Gaussian-type PSF. The pulse length

$$\mathrm{PSFs}=\begin{cases} \exp\{-(\frac{x^2}{2\sigma_x^2}+\frac{y^2}{2\sigma_y^2})\}\cos(2\pi\frac{x}{\frac{\lambda}{2}}) & \text{Gaussian-type;} \\ A\cdot\cos(2\pi\frac{x}{\frac{\lambda}{2}}) \quad \text{if } A>0 & \\ \quad\text{where } A=-\frac{8}{9\pi}[(\frac{x}{\sigma_x})^2+(\frac{y}{\sigma_y})^2]+1 & \text{Parabolic type;} \\ \cos(2\pi\frac{x}{\frac{\lambda}{2}}) \quad \text{if } (\frac{x}{\sigma_x})^2+(\frac{y}{\sigma_y})^2\le\frac{9\pi}{8} & \text{Rectangular type.} \end{cases}$$

and the beam width of the rectangular type PSF was made same as the parabolic type PSF. For the Gaussian-type PSF, the respective axial (x) and lateral (y) standard deviations (σ_x and σ_y) were set to 0.2mm. To yield valuable echo data for the DLs, large steering and coherent superposition were performed for the transmission and reception. In addition to in the frontal direction at 0 degrees (i.e., depth direction), 4 steering angles were made, i.e., from 10, 20, 30 to 40 degrees symmetrically with respect to the depth direction.

For the attenuation map estimation, attenuated echo data were simulated with the Gaussian-type PSF according to the Lambert's law. The attenuation coefficients of ultrasound were set to 0.5 to 0.7 dB/MHz·cm randomly in a circular region of 5 mm in diameter and the surrounding, respectively.

2.2 Deep learning setting

In the supervised setting, we trained on (i) the reflection coefficients and scattering coefficients (i.e., inverse filtering), (ii) and (iii) one of them, (iv) specular (i.e., speckle reduction), and (v) speckle. Thus, the superresolution and/or separation was performed about the reflection and scattering phenomena. And, in the unsupervised setting, we performed speckle reduction[1]. The number of data samples for both supervised and unsupervised learning was 1000; the respective epochs were 300 and 50, and the respective batch sizes were 8 and 20; and the learning rate was 0.001 for both cases.

For the attenuation map estimation, a tentative result will be shown later.

3. Results

Figs. 1a and **1c** respectively show the results except for the attenuation results, obtained for the Gaussian- and rectangular PSF echo data (parabolic results omitted). The supervised model succeeded in both the superresolution and the

E-mail: †*c-sumi@sophia.ac.jp

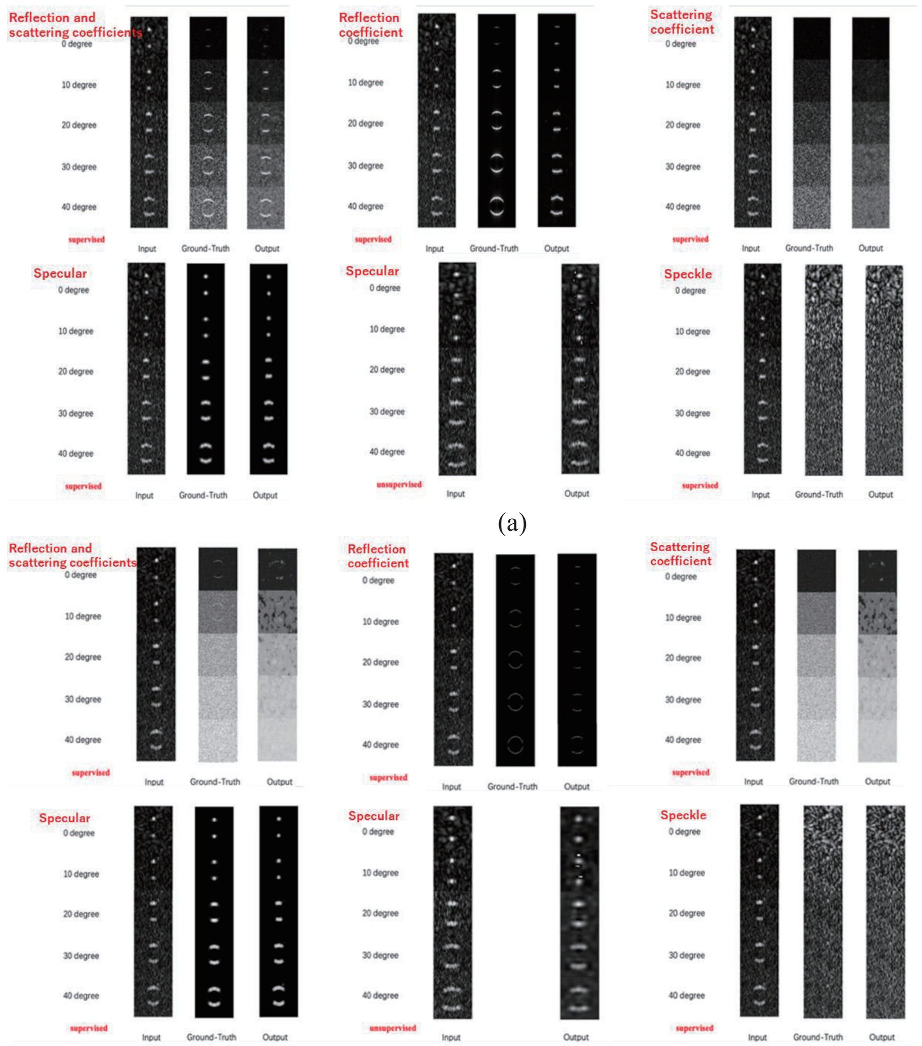

(a)

(b)

Fig. 1. Results of superresolution and separation for (a) Gaussian and (b) rectangular PSF data.

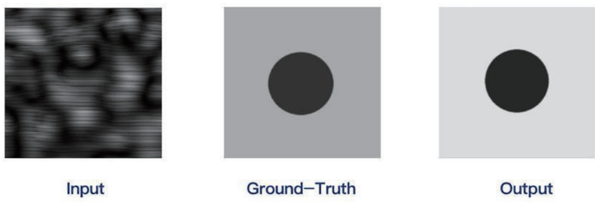

Fig. 2. Estimation of attenuation coefficient map.

separation. For rectangular and parabolic PSF data yielded higher spatial resolutions than the Gaussian PSF data, actually, rectangular > parabolic > Gaussian-type images.

Particularly, regarding the superresolution, we had also confirmed the effects generated with the PSF types through the digital signal processing of inverse filtering in spatial and frequency domains previously. Specifically, however, the DLs did not performed perfectly with respect to the scattering echo data, i.e., when yielding a mixture of reflection and scattering coefficients as well as the scattering coefficients solo. The performance with respect to the specular echo data were excellent considerably.

Regarding the separation about the specular and speckle, the supervised model performed well considerably. The supervised model had the higher speckle removal ability than the unsupervised model.

Fig. 2 shows a tentative result of the attenuation coefficient map estimated, which still had less accuracy about the attenuation coefficient values.

4. Conclusions

The basic supervised-type CNN model was able to perform the superresolution excellently particularly for the specular echo data; and the separation of specular and speckle echo data. The speckle reduction was intense than that of unsupervised model. The possibility of estimating attenuation maps with the CNN model has also been confirmed, but so far it seems that a sophisticated model is needed. In the near future, we'll compare the performance with those of our previously applied models in detail; and develop new models.

References

1) Y. Li, M. Zhang, G. Ogane, C. Sumi. Proc 44th Ann Int Conf IEEE Eng Med Biol Soc (EMBC), 2022, pp. 2088-2092.
2) M. Zhang, Y. Li, C. Sumi, Proc USE 2021, 2Pa5-4.
3) S. Li, M. Zhang, Y. Li, C. Sumi. Segmentation with speckle reduction and superresolution by deep leaning for human ultrasonic echo image. Proc 43rd EMBC, 2021, pp. 3663-3667.